Colloids and Surfaces A: Physicochem. Eng. Aspects 345 (2009) 18–25

Contents lists available at ScienceDirect

Colloids and Surfaces A: Physicochemical and Engineering Aspects

journal homepage: www.elsevier.com/locate/colsurfa

# Gradient distribution of fluorine on the film surface of the organic–inorganic hybrid fluoropolymer

Ailan Qu[a,*], Xiufang Wen[b], Pihui Pi[b], Jiang Cheng[b], Zhuoru Yang[b]

[a] Department of Chemistry, Jinan University, Guangzhou 510632, China
[b] The School of Chemical and Energy Engineering, South China University of Technology, Guangzhou 510640, China

ARTICLE INFO

*Article history:*
Received 15 August 2008
Received in revised form 16 March 2009
Accepted 21 March 2009
Available online 28 March 2009

*Keywords:*
Fluorocopolymer
Preferential migration
Emulsion polymerization
Hybrid polymers

ABSTRACT

Inorganic–organic hybrid latex containing fluoride has been prepared in multistage emulsion polymerization in the presence of nano-$SiO_2$ particles and alkoxysilane (γ-methacryloxypropyltri(isopropoxy)silane, MAPTIPS). The effects of fluoride and alkoxysilane on the morphologies of composite particles were observed and it was found that the encapsulation may be fulfilled in the presence of dodecafluoroheptyl methacrylate together with MAPTIPS whether using raw $SiO_2$ particles or modified. The distribution of fluorine in different latex films was measured by X-ray photoelectron spectroscopy. It was indicated that the gradient distribution of fluorine from depth profile in the films may be enhanced by MAPTIPS and encapsulated $SiO_2$ due to the bidirectional move of MAPTIPS and congregation of $SiO_2$ on the film surface. Combining the results of XPS with AFM analysis, it was showed that the phase separation between organic and inorganic for encapsulated $SiO_2$ was lightened, while it was so apparent for raw $SiO_2$ that the orientation to the surface of fluorine was restrained in the lack of MAPTIPS.



## 1. Introduction

Formation of surface functional films using fluoropolymer has been a topic of numerous studies owing to their attractive properties such as low surface energy, heat resistance, chemical inertness, and low dielectric constant [1]. As we all know, surface energy is the dominant factor to determine the wettability and adhesion of coatings. It is often desirable to combine the bulk properties of the coatings with specific surface properties to achieve a film with good comprehensive performance. Therefore, acrylic copolymers made of hydrocarbon and fluorocarbon monomers are commonly used to prepare low surface energy systems because they have a good reactivity and fluorinated monomers are effective in low-surface energy modification due to surface accumulation of fluorine atoms [2]. Furthermore, alkoxylsilane is also used to improve adhesion which serves as an anchor to the substrate with hydroxyls by forming covalent bonds [3]. On the other hand, the incorporation of an inorganic phase into an organic polymer matrix may be an effective approach to increase mechanical strength and provide improvements in other specific properties of organic polymer [4]. Organic–inorganic hybrids which combine the advantages of several materials and exhibit multifunctional characteristic, have been developed as binders for aqueous coatings. Heterogeneous polymerization, especially emulsion polymerization, provides an effective way and is by far the most frequently used technique.

Fluorinated materials are capable of self-migration to the surface and self-assembling of their fluorine atoms. It was observed that the concentration profile of fluorine in the films exhibited a gradient to the surface [5,6], nevertheless, up to date, very few papers have reported the case of the composite latex based on fluoropolymer [7]. In this experiment, we used acrylate monomers in an aqueous system modified with γ-methacryloxypropyltri(isopropoxy)silane (MAPTIPS) to improve adhesion and solvent resistance, with nanosilica particles to increase hardness and mechanical strength, as well as a fluorinated monomer to improve hydrophobicity. Because of the presence of nanoinorganic particles, multiple interfaces, and a wide range of components used, latex systems were heterogeneous and phase separation can be induced. In this paper, the influences of fluoride or alkoxysilane on the morphology of composite particles, and the effects on the gradient distribution of fluorine in the formation of latex films resulted from the presence of MAPTIPS and inorganic silica ($SiO_2$) particles were discussed.

## 2. Experimental

### 2.1. Materials

The monomer of γ-methacryloxypropyltri(isopropoxy)silane (MAPTIPS, $CH_2{=}C(CH_3)COO(CH_2)_3Si(OC_3H_7)_3$) was obtained from Acros Organics Co. in USA. The hydrophobic monomers of hexaflu-

* Corresponding author. Tel.: +86 013710228756.
*E-mail addresses:* qal67@163.com, Aileenqal@yahoo.cn (A. Qu).

0927-7757/$ – see front matter © 2009 Published by Elsevier B.V.
doi:10.1016/j.colsurfa.2009.03.035

orobutyl acrylate (HFBA, $CH_2$=$CHCOOCH_2CF_2CHFCF_3$) and dodecafluoroheptyl methacrylate (DFMA, $CH_2$=$C(CH_3)COOCH_2CF(CF_3)CHFCF(CF_3)_2$) were supplied by XEOGIA Fluorine-Silicon Chemical Co. Ltd., in China. The anionic surfactant of allyloxy polyoxyethylene(10)nonyl ammonium sulfate (DNS-86) was from Shuangjian Co. Ltd. in Guangzhou of China. The other chemicals were purchased in their reagent grade and used without further purification including methyl methacrylate (MMA, 97%), butyl acrylate (BA, 96%), 2-hydroxyethyl methacrylate (HEMA, 98%), α-methyl acrylic acid (MAA, 98%), sodium hydrogenocarbonate ($NaHCO_3$), potassium persulfate (KPS), nonylphenol poly(oxyethylenic) ether (OP-10), methacryloxypropyltrimethoxysilane (MATMS), tetraethoxysilane (TEOS), ethanol ($C_2H_5OH$), and ammonia ($NH_4OH$, 30% in water). Deionized water was prepared for all polymerization and treatment process.

### 2.2. Preparation and modification of $SiO_2$ particles

Silica particles were prepared according to well-known Stöber method [8] which is very convenient to manipulate the particle size. A 500 mL of absolute ethanol and 24 mL aqueous solution of ammonia were introduced in a 1000-mL, three-neck, round-bottom flask equipped with a heat exchange system. The mixture was stirred at 300 rpm to homogenize and heated at 60 °C. After stabilization, 15 mL of TEOS was added into the solution and reaction occurred at the chosen temperature with constant stirring for 24 h to get silica of about 78 nm diameter. The modification of the silica beads was carried out by adding MATMS directly into the particles dispersion. The amount of coupling agent was 0.3 g/g $SiO_2$. After the mixture was stirred for 12 h at ambient temperature, the reaction medium was heated to 80 °C for 1 h to promote covalent bonding of the organic silane to the surface of the silica nanoparticles [9]. When the synthesis of silica particles was completed, the main part of ethanol and ammonia was first removed through evaporation under reduced pressure and the ethanol in resulting suspension was replaced with water. The content of ethanol is about 5–10% based on the weight of water. And it was controlled by adding water on the basis of calculating the content of ethanol according to the weight of raw materials, change of suspension and additive water. In order to ensure the equal content of ethanol, the same passel of silica suspension was used in the contrastive experiments.

### 2.3. Preparation of hybrid latex

The latex particles were prepared by using a multi-stage emulsion polymerization technique. For the synthesis of composite particles using either modified or unmodified silica particles as core, the given amount of dealt silica suspension (a mixture of water and ethanol containing surfactant OP-10 and DNS-86) was transferred into a thermostated reactor with continuous stirring. Part of MMA was added to the 2.0 g of water solution with surfactants (0.25 g of OP-10 and 0.2 g of DNS-86 dissolved in 12 g water as solution A) and emulsified for 20 min with magnetic stirring. Then it was added dropwise, together with part of initiator KPS dissolved in water. After the reaction was kept for 30 min, a pre-emulsified mixture of MMA, BA, HEMA, and α-MAA, and then the pre-emulsified mixtures of MMA, BA, DFMA or HFBA and MAPTIPS were added subsequently. Detailed recipes given in Table 1 summarized a series of experiments. The polymerization started at 75 °C and finished within 8 h. It was necessary to control the pH value of initial dispersion (pH 7.5) by using the buffer ($NaHCO_3$) since nanosilica particles show acidic character in the aqueous dispersion. It is the same as above for the preparation of fluorinated acrylic copolymer without $SiO_2$ particles except replacing $SiO_2$ suspension with water medium.

### 2.4. Characterization

The size and distribution of silica and composite latex particles were determined by Laser Diffraction Particle Size Analyzer (ZS Nano S) from Malvern Co. in England. The morphologies of composite particles were characterized by transmission electron microscopy (TEM), which could also show approximately the thickness of the shells for core–shell particles. TEM measurements were performed on Tecnai 10 (Holand, Philips Co.) microscope at an accelerator voltage of 200 kV. One drop of the suspension was diluted into water and placed on a carbon-coated copper grid to be stained with phosphato-tungstic acid ($H_3[P(W_3O_{10})_4]\cdot 14H_2O$) for 30 s and dried in air before observation. The Fourier transform infrared spectrometer (FTIR) (VECTOR 33, Bruker Co. of Germany) was carried out to determine the chemical structure of latex. The latex particle was separated by centrifugation, mixed with KBr, and pressed into pellets before the spectra were recorded. The adsorbed or grafted polymer content was determined as follows: the latex was first centrifuged to separate the serum, and then dried under vacuum. Toluene extraction for 8 h under reflux by Soxhlet extraction allows dissolution of the polymer that is simply adsorbed; the residual solid is the silica covered with grafted polymer [10]. The amount of bonded polymer was determined by difference in weight between the total and the extracted free polymer. The amount of total polymer or silica was obtained by the thermogravimetrical analyzer (TG/DSC, STA449C) from NETZSCH Co. in Germany by heating the sample (8 mg) in a flow of nitrogen (30 mL/min) at 10 °C/min from room temperature to 700 °C.

The latex film was prepared by coating on glass slides to be dried at room temperature for over 2 days and nights. Contact angle for water (WCA) was measured with an OCA15 contact angle goniometer from Dataphysics Co. in Germany. The liquid droplet volume is 2 μL. Typically, measurements were collected for five drops across the surface. X-ray photoelectron spectroscopy (XPS) data were collected in both survey and high-resolution mode on Krafos Axis Ultra DCD systems equipped with a Al Kα source and operating at 150 W. Scanning scope is 700 μm × 300 μm. Data was recorded at 20°, 40°, 60° and 90° takeoff angles. Semi-quantification was done by integration of the atomic signals and corrected with sensitivity factors adjusted for the instrument lens and detector design. Spectra were then charge-corrected to align the hydrocarbon component of the $C_{1s}$ region to 285.0 eV. Atomic force microscopy (AFM) was performed using a Dimension 62000nm instrument (CSPM2000). Images were acquired under ambient conditions in tapping mode using a Nanoprobe cantilever.

## 3. Results and discussion

### 3.1. Effects of fluoride and alkoxysilane on microstructure of composite particles

The latex particles were prepared by a three-stage semi-continuous emulsion polymerization under the same controlled conditions as described in Section 2. The typical morphologies of different particles shown by TEM were given in Fig. 1 and the mean sizes of resulting particles listed in Table 1 were coincident with the TEM images. Fig. 1a and b represents the latex particles containing DFMA and MAPTIPS of recipe 4 with 107 nm mean diameter and silica particles with 78 nm mean diameter made by Stöber method. The morphology of composite particles prepared according to recipe 5 in the absence of fluoride and alkoxysilane was characterized in Fig. 1c. The raw silica beads were completely covered with polymer having an irregular contour. It might originate from the free molecules of monomers that were first nucleated in the continuous phase and soon after hetero-coagulated on the silica surface forming a shell at the end of the polymerization, just

**Table 1**
Recipes used in the experiments[a].

| | Recipe no. | | | | | | | |
|---|---|---|---|---|---|---|---|---|
| | 1 | 2 | 3 | 4 | 5 | 6 | 7 | 8 |
| Medium[b] | 80 | 80 | 80 | 80 | 80 | 80 | 80 | 80 |
| OP-10 | 0.12 | 0.12 | 0.12 | 0.12 | 0.25 | 0.25 | 0.25 | 0.25 |
| DNS-86 | 0.1 | 0.1 | 0.1 | 0.1 | 0.2 | 0.2 | 0.2 | 0.2 |
| Raw silica | – | – | – | – | 6.0 | 6.0 | 6.0 | |
| Modified silica | – | – | – | – | – | – | | 6.0 |
| $NaHCO_3$ | 0.2 | 0.2 | 0.2 | 0.2 | 0.5 | 0.5 | 0.5 | 0.5 |
| First stage | | | | | | | | |
| MMA | 3.0 | 3.0 | 3.0 | 3.0 | 3.0 | 3.0 | 3.0 | 3.0 |
| Solution A | 2.0 | 2.0 | 2.0 | 2.0 | 2.0 | 2.0 | 2.0 | 2.0 |
| KPS + water | 0.02 + 2.0 | 0.02 + 2.0 | 0.02 + 2.0 | 0.02 + 2.0 | 004 + 2.0 | 004 + 2.0 | 0.04 + 2.0 | 0.04 + 2.0 |
| Second stage | | | | | | | | |
| MMA | 4.0 | 3.4 | 2.6 | 1.8 | 3.0 | 2.6 | 1.8 | 1.8 |
| BA | 4.2 | 3.6 | 3.8 | 3.0 | 3.6 | 3.8 | 3.0 | 3.0 |
| MAA | 0.4 | 0.4 | 0.4 | 0.4 | 0.4 | 0.4 | 0.4 | 0.4 |
| HEMA | 0.4 | 0.4 | 0.4 | 0.4 | 0.4 | 0.4 | 0.4 | 0.4 |
| Solution A | 2.5 | 2.5 | 2.5 | 2.5 | 2.5 | 2.5 | 2.5 | 2.5 |
| KPS + water | 0.04 + 3.0 | 0.04 + 3.0 | 0.03 + 2.0 | 0.03 + 2.0 | 0.06 + 2.0 | 0.06 + 2.0 | 0.06 + 2.0 | 0.06 + 2.0 |
| Third stage | | | | | | | | |
| MMA | 1.0 | 1.0 | – | – | 3.6 | – | – | – |
| BA | 1.0 | 1.0 | 1.8 | 1.8 | 6.0 | 1.8 | 1.8 | 1.8 |
| HFBA | 6.0 | 6.0 | – | – | – | – | – | – |
| DFMA | – | – | 8.0 | 8.0 | – | 8.0 | 8.0 | 8.0 |
| MAPTIPS | – | 1.2 | – | 1.6 | – | – | 1.6 | 1.6 |
| Solution A | 7.0 | 7.0 | 7.5 | 7.5 | 7.5 | 7.5 | 7.5 | 7.5 |
| KPS + water | 0.04 + 3.0 | 0.04 + 3.0 | 0.05 + 4.0 | 0.05 + 4.0 | 0.10 + 4.0 | 0.10 + 4.0 | 0.10 + 4.0 | 0.10 + 4.0 |
| Mean particle size (nm) | 116 | 101 | 122 | 107 | 142 | 98 | 191 | 123 |
| Polydispersity index | 0.108 | 0.096 | 0.117 | 0.102 | 0.185 | 0.346 | 0.186 | 0.150 |
| Average theoretical fluorine content | 13.9 | 13.9 | 21.9 | 21.9 | 0 | 16.5 | 16.5 | 16.5 |

[a] All reported amounts are in gram except polydispersity index and especially marked.
[b] The medium was deionized water for recipes 1–4 and it was admixture of water and ethanol for recipes 5–8.

as approach 1 shown in Scheme 1. In this case, the average size of the core–shell particle was 142 nm and 30–50 nm for the shell thickness. When the fluoride was used instead of part of acrylates as recipe 6 at the same conditions of recipe 5 reported in Table 1, it was unsuccessful to obtain core–shell particles. Instead, only partial coverage with latex particles surrounding the inorganic seed was observed, as shown in Fig. 1d. This is due to lack of compatibility at the interface between strong hydrophilic silica particle surface and hydrophobic monomers and polymer nuclei which led to unsuccessful encapsulation [10]. However, when the MAPTIPS was used together with DFMA and acrylates in the same experimental conditions (recipe 7), the composite particles with two different morphologies forming irregular core–shell (sandwich-shape and strawberry-like) structure for raw silica seeds were obtained as illustrated in Fig. 1e. By comparison, the morphologies of the composite particles prepared in the presence of the silica modified with MATMS were observed that almost each composite particle with 123 nm mean diameter containing silica formed snowman-like or sandwich-shape of Fig. 1f (recipe 8). Before DFMA and MAPTIPS were added in the multistage polymerization, the reaction may be occurred as approach 1 in Scheme 1, individual polymer particles (formed in the earlier stages of the polymerization) coagulating on the silica surface. Since the time of polymerization was short and dosage of monomers in first step decreased, there were two kinds of $SiO_2$ shapes in the reaction system during this period which were bare silica particles and composite particles encapsulated with primary latex particles. When DFMA and MAPTIPS were introduced, the MAPTIPS molecules with a strong affinity for the silica surface hydrolyzed rapidly to form silanols which associate to give oligomers ultimately to condense on the bare silica surface like the polymerization with modified silica particles as seeds. The mechanisms may be elucidated as approach 2 in Scheme 1. The copolymerization between free molecules of monomers and the methacryloxy groups of alkoxysilane formed oligomers which are expected to be strongly entangled between themselves and around the silica compactly [10], leading the formation of a polymer shell. However, the incompatibility between silica and polymer increased in the presence of the fluoroacrylate and it is easy to result in the phase separation which leads to the formation of irregular core–shell composite particles, like snowman-like or sandwich. The detail mechanism of encapsulation and factors on morphologies of composite particles were discussed in elsewhere [11].

### 3.2. Analysis of chemical structure

The FTIR was used to characterize their chemical structure. The FTIR spectrum of the sol–gel silica particles (curve a), pure emulsion (recipe 4, curve d) and composite latex (recipes 7 and 8, curves b and c) were shown in Fig. 2, respectively. It can be seen that the FTIR spectrum of composite latex had all the characteristic bands of nanosilica and pure polyacrylate latex. Comparing with curve d, the characteristic peaks of Si–O–Si bond in the composite latex increased its intensity indicating the successful incorporation of silica in the hybrid films. In addition, the absorption represented in the carbonyl bonding is slightly different in the pure polyacrylate latex and composite latex. The peak of the C=O stretching vibration shifts from 1730 $cm^{-1}$ in the pure polyacrylate latex to 1740 $cm^{-1}$ because of the effect of the intra-molecular hydrogen bonding between the nanosilica and polyacrylate chains. From the difference in the FTIR spectra between the pure polyacrylate latex and the composite latex and the difference of measured graft ratio (79 wt.% of the total amount of polymer surrounding the silica beads was grafted, whereas 21% was dissolved and for the modified silica

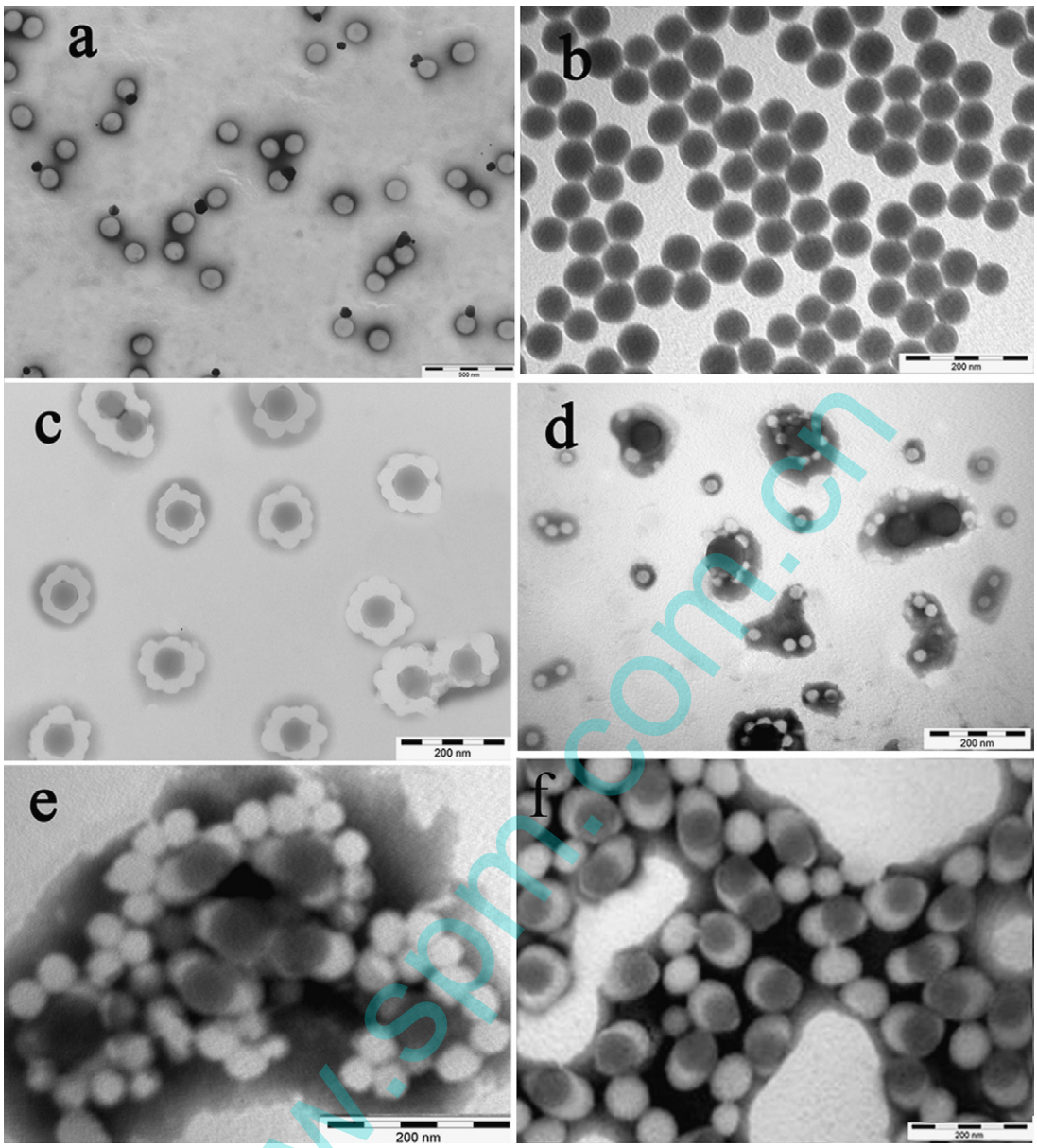


**Fig. 1.** TEM images of different particles (a, acrylates latex particles containing DFMA and MAPTIPS; b, silica; c, raw silica/acrylates composites; d, raw silica/ acrylates composites containing DFMA; e, raw silica/ acrylates composites containing DFMA and MAPTIPS; f, modified silica/ acrylates composites containing DFMA and MAPTIPS).

particles, the grafted polymer was 86% and non-grafted polymer was 14%), it could be concluded that strong inter-molecular chemical bonding tethered the nanosilica and polyacrylate chains in the composite film [12].

Since the fluorine groups cannot be identified clearly by FTIR, it was necessary to characterize structurally them in the composite latex by the XPS analysis. The spectrum of survey and carbon for DFMA were given in Fig. 3. Comparing the binding energies and spectra between two samples of recipes 2 and 4, both of them are similar with respect to $F_{1s}$, $O_{1s}$ and $C_{1s}$. Discerning the chemical make-up of the $F_{1s}$ and $O_{1s}$ windows was straightforward. The $F_{1s}$ window in both samples showed a singular symmetrical peak at $688.8 \pm 0.05$ eV, and the $O_{1s}$ window showed two peaks with similar areas at $533.4 \pm 0.1$ and $531.9 \pm 0.05$ eV, respectively, corresponding to the two different types of oxygen in the ester functional group. The $C_{1s}$ window showed a complex pattern of peaks extending over about 8.6 eV range between 285.0 and 293.6 eV. A typical $C_{1s}$ spectrum of recipe 4 which stands for four kinds of carbon bonds was given in Fig. 3b. The peaks of binding energy at 293.8, 286.4 and 285.0 eV are corresponding to the bonds of $CF_3$, C–O and C–C, respectively. The binding energy of any CF groups (ca. 289.6 eV) would essentially be indistinguishable from that of C=O (289.4 eV), resulting in peak overlapping. When HFBA was used in recipe 2, the $C_{1s}$ windows showed five kinds of peaks because of increase of $CF_2$ groups between CF and $CF_3$ peak. These agree well with previously published literature and reference values on fluorinated as well as acrylic polymers [13,14]. There was also a peak of $Si_{2p}$ corresponding to Si–O at 101.6 eV due to the hydrolysis and condensation of MAPTIPS. These results showed that the fluoromonomers have participated in the reaction and the chemical environment of atoms F, O and Si to be alike in both cases apart from C atom.

Comparing the binding energy data of samples 7 and 8 with that of sample 4, it was shown that the binding energies of $C_{1s}$ in samples 7 and 8 became a little higher due to the presence of MAPTIPS together with $SiO_2$. Besides this, chemical shift of the binding energy $Si_{2p}$ for Si–O group was induced by MAPTIPS or the presence of silica in samples 7 and 8. This fact implied that the cross-linking density increased in the coactions of MAPTIPS and $SiO_2$. The bind-

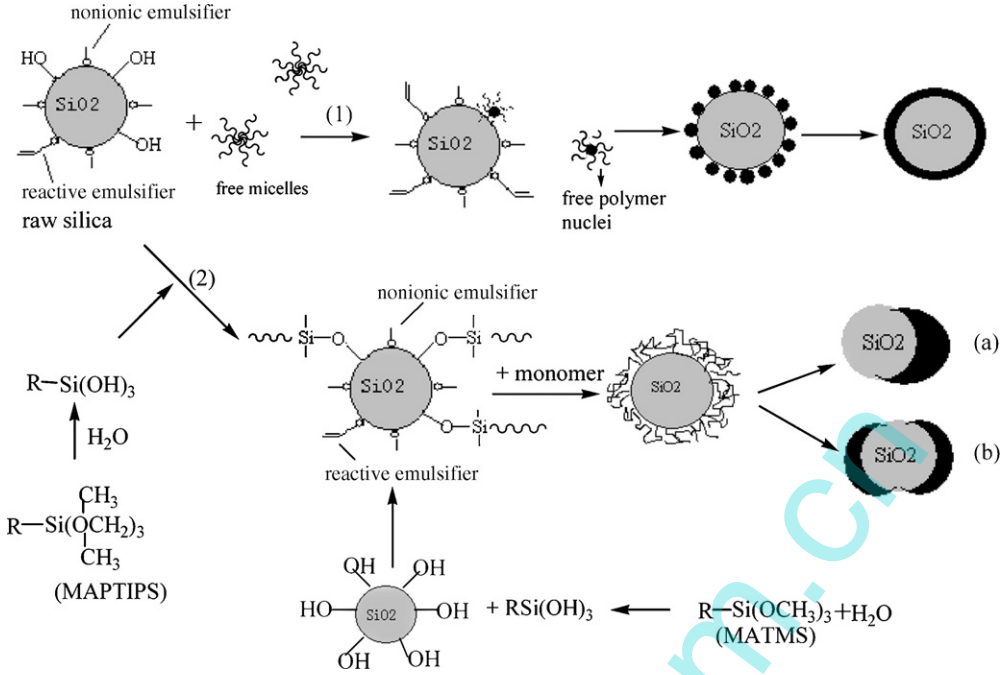


**Scheme 1.** The schematic illustration of the formation of composite particles by emulsion polymerization.

ing energies of $F_{1s}$ and $O_{1s}$ in recipes 7 and 8 are all the same as that in recipe 4 (Table 2).

### 3.3. Effect of MAPTIPS on gradient of fluorine

It has been known that fluorinated materials are capable of self-migration to the surface. Since the composition of the surface is a critical feature of these polymers, an attempt was made to find out the distribution of fluorine in the film and the effect of MAPTIPS on it by using the XPS spectra which is the most widely employed method for quantitative analysis of surface compositions. Analyses performed at various take-off angles of 20°, 40°, 60° and 90° provided a means to probe both the surface and deeper features of these materials. The results of XPS were shown in Table 3. Recipes 1 and 3 are the films containing HFBA and DFMA in shell, respectively. Recipes 2 and 4 are both added MAPTIPS in the shell together with fluoromonomer at the same content of fluorine as recipes 1 and 2. As can be seen from Table 3, in all cases, the fluorine content on the layer of the outmost surface is higher than that on the layer near the bulk (average theoretical fluorine content was shown in Table 1) and it decreases along with depth into the film, while carbon is contrary. This indicated, as anticipated, that the fluorocarbon side chain enriched preferentially on the surface compared to the acrylate backbone and a gradient of fluorine existed from surface to the bulk of polymer film. The data of recipe 2 showed clearly that the fluorine content in each layer at the same takeoff angle is higher than that in recipe 1. The same phenomenon was shown in recipes 3 and 4. The water contact angle (WCA) on film surface may reflect the hydrophobic compositions on the other hand. The WCA on the film surface of recipe 1 was only about 65°, while the WCA increased to 95° when 6.0 wt.% MAPTIPS (based on the total amount of monomers) was added together with HFBA in the shell. When DFMA was used to replace HFBA at the same content, the WCA increased to 96° approximately and it was improved to 106° when MAPTIPS was added together even though the improved result was not so apparent as that of HFBA.

Combining the results of XPS and WCA, they suggested that the MAPTIPS may promote a larger gradient distribution of fluorine concentration from the depth profile in the film. Polymer compatibility can play a substantial role in determining the distribution of fluorine in the film. Not only will the different types of poly-

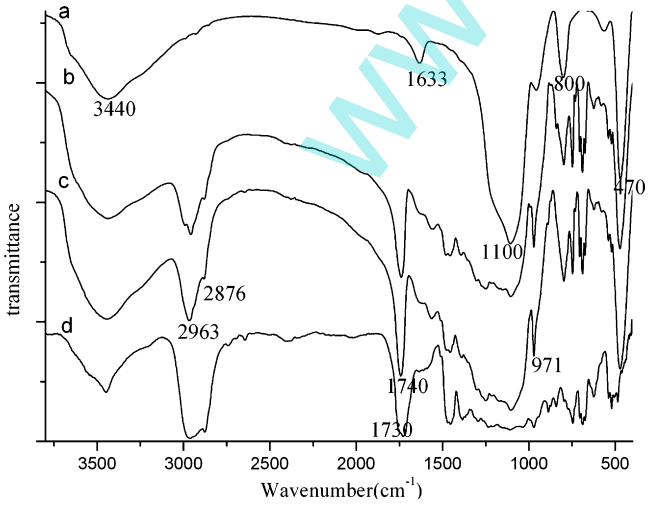


**Fig. 2.** FTIR spectra of particles (a, raw silica; b, raw silica/DFMA–MAPTIPS–acrylates composites; c, modified silica/ DFMA–MAPTIPS–acrylates composites; d, DFMA–MAPTIPS–acrylates latex).

**Table 2**
Binding energies (Eb) of different functional groups.

| Atom | Functional group | Sample 4 Eb (eV) | Sample 7 Eb (eV) | Sample 8 Eb (eV) |
|---|---|---|---|---|
| $C_{1s}$ | $CF_3$ | 293.5 | 294.0 | 293.9 |
| | C=O | 289.3 | 289.6 | 289.8 |
| | C–O | 286.4 | 286.6 | 286.6 |
| | $-CH_2-C$ | 285.0 | 285.0 | 285.0 |
| $Si_{2p}$ | Si–O | 101.6 | 102.0 | 102.7 |
| $F_{1s}$ | C–F | 686.8 | 686.7 | 686.8 |
| $O_{1s}$ | C=O | 533.9 | 534.6 | 534.2 |
| | C–O | 532.4 | 532.6 | 532.6 |

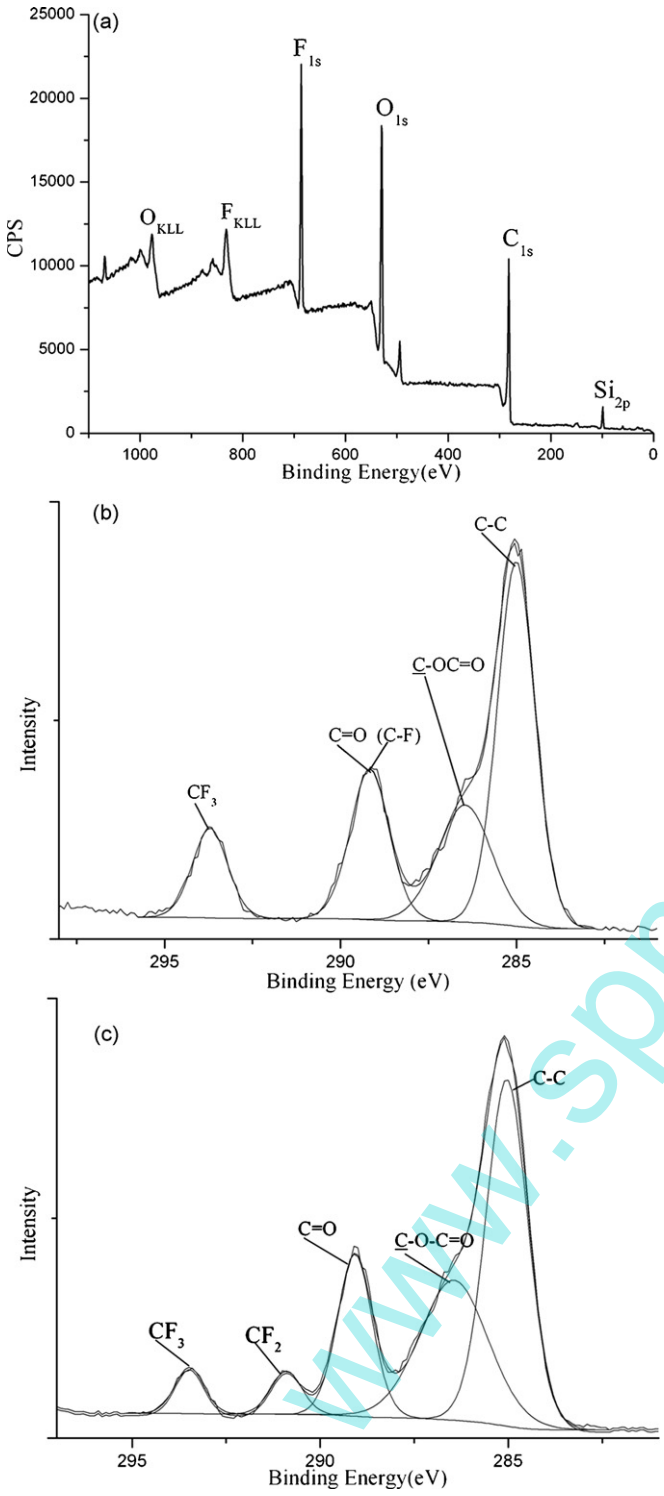


**Fig. 3.** The XPS spectra of latex films (a, survey; b, $C_{1s}$ spectrum of recipe 4; c, $C_{1s}$ spectrum of recipe 2).

mer chains synthesized have a different chemical potential, but also they will have different polymer–polymer interaction parameters which will determine the extent of their compatibility. Both of these factors become important in determining the distribution of fluorine at the interface [5]. In the system of recipe 1, the separation is governed by the repulsion between the fluoroalkyl-chain and the alkyl-chains [15]. The driving force of phase separation for HFBA is weak and it is difficult for fluorine to orientate on the surface because of too short chain of fluoroacrylate and similar reactivity with acrylates. This resulted in the fluorine having a slight bias for the surface and a low contact angle. While for the sample 2 or 4, the possible reason is that the MAPTIPS has a similar property of propensity on the surface and also serves as an anchor to the substrate by forming covalent bonds, making it possible for MAPTIPS to provide a channel benefit for fluorine migrating to the film surface. The compositions of the surface and the different layer showed that self-assembly has successfully introduced hydrophobic groups to form a gradient functional distribution which can be influenced by the addition of MAPTIPS.

### 3.4. Effect of $SiO_2$ particles on fluorine orientability

In previous reports of preparing hybrid emulsion, silica particles are usually modified by silicane coupling agent in order to improve the dispersibility and stability in organic monomers phase [3]. This may depress the incompatibility between $SiO_2$ and organic phase. Additionally, using an organic polymer with the ability to form hydrogen bond with the silanol on the inorganic particle surface can also retard phase separation and result in homogeneous systems. To achieve a low surface free energy, however, the surface of materials needs to be covered with perfluoroalkyl groups through surface segregation and phase separation. For the sake of understanding the influence of $SiO_2$ particles on the distribution of fluorine in hybrid film, the gradient of fluorine in composite films was observed. The results examined by XPS were shown in Table 4. Raw $SiO_2$ particles were introduced in sample 7 on the base of recipe 4. The films of recipe 8 showed the results in the presence of modified silica particles. Comparing the gradient changes of fluorine aroused by MAPTIPS and $SiO_2$ from these samples, it was shown that MAPTIPS still improved the ability of fluorine moving to the surface and the fluorine content on the surface also increased in the presence of $SiO_2$ particles. At the same time, by comparing the fluorine contents in recipes 7 and 8 with that in recipe 4, it was also concluded that the aggregation of fluorine on the surface may be impervious in the coexistence of MAPTIPS and $SiO_2$ whether it was modified or not (even though the data of fluorine in Table 4 for recipes 7 and 8 was lower than that of recipe 4, it was said to be relative increased by the theoretical fluorine content). Considering the structure of hybrid latex particles, the raw and modified $SiO_2$ particles were encapsulated to be homogeneous so that there is no obvious difference of fluorine distribution. For the sample 8 with modified $SiO_2$, the silicon content on the surface is higher, indicating that the modifier MTMAS has taken part in the polymerization and silica particles may be present on the film surface which cannot be confirmed for raw silica due to the encapsulation by polymers. However, from the results of recipes 6 and 3 in the

**Table 3**
The elements content in the films from XPS.

| Takeoff angle (°) | Recipe 1 (atom%) | | | Recipe 2 (atom%) | | | | Recipe 3 (atom%) | | | Recipe 4 (atom%) | | | |
|---|---|---|---|---|---|---|---|---|---|---|---|---|---|---|
| | F | C | O | F | C | O | Si | F | C | O | F | C | O | Si |
| 20 | 17.0 | 62.7 | 20.3 | 21.9 | 58.2 | 19.3 | 0.5 | 25.3 | 59.5 | 14.8 | 28.7 | 59.1 | 10.5 | 1.6 |
| 40 | 16.1 | 63.2 | 20.7 | 19.8 | 59.9 | 19.9 | 0.3 | 23.9 | 61.0 | 15.1 | 27.4 | 58.3 | 13.1 | 1.1 |
| 60 | 15.7 | 64.6 | 19.7 | 19.2 | 60.6 | 19.6 | 0.5 | 23.2 | 62.1 | 14.3 | 26.3 | 58.1 | 14.2 | 1.4 |
| 90 | 15.3 | 65.0 | 19.7 | 18.0 | 61.4 | 19.9 | 0.6 | 22.1 | 63.0 | 14.7 | 22.5 | 61.4 | 14.5 | 1.5 |

**Table 4**
The element contents in the films from XPS.

| Takeoff angle (°) | Recipe 6 (atom%) | | | | Recipe 7 (atom%) | | | | Recipe 8 (atom%) | | | |
|---|---|---|---|---|---|---|---|---|---|---|---|---|
| | F | C | O | Si | F | C | O | Si | F | C | O | Si |
| 20 | 18.3 (24.3) | 56.1 | 20.4 | 3.5 | 23.5 (31.2) | 54.3 | 20.5 | 1.3 | 23.0 (30.6) | 54.0 | 20.2 | 2.7 |
| 40 | 17.1 (22.7) | 60.3 | 19.8 | 2.7 | 22.6 (30.0) | 54.8 | 20.9 | 1.1 | 22.4 (29.8) | 54.3 | 20.1 | 2.6 |
| 60 | 15.4 (20.5) | 62.5 | 20.1 | 1.9 | 18.0 (23.9) | 63.3 | 17.5 | 1.0 | 17.5 (23.3) | 63.0 | 17.3 | 2.1 |
| 90 | 16.9 (22.5) | 58.9 | 19.6 | 2.5 | 22.8 (30.3) | 56.5 | 19.3 | 1.3 | 22.6 (30.0) | 54.1 | 20.4 | 2.6 |

*Note*: The data in parenthesis was calculated based on the same mass content of recipe 4.

absence of MAPTIPS, it was shown that the percentage of fluorine on the film surface of recipe 6 decreased while the content of silicon increased. It is indicated that silica particles inhibit the migration and enrichment of fluorine-containing chain segments toward the surface. The results were consistent with that of WCA. When the silica particles were added in the presence of MAPTIPS, the water contact angle on the film surface increased from 106° to about 135°. But it decreased slightly when silica particles were added in the lack of MAPTIPS. The difference may be dependent on the failed encapsulated structure of composite particles which resulted in the $SiO_2$ particles to be easily separated from organic polymer particles due to phase separation [16]. The incompatibility between silica and organic polymer restrains the tendency to the surface of fluorine because of the strong hydrophilicity of silanol groups on surface of raw $SiO_2$ congregating on the top layer of film. This will be verified by the AFM characterization in the later.

It is important to note that for all the samples containing $SiO_2$ particles in despite of being modified or unmodified, the gradient of fluorine occurred only on the depth detected by takeoff angles from 20° to 60°, which implied the atomic percentage of fluorine drops from its high level at the surface to low concentration with a sharp profile that extends only over a thin depth. The difference of fluorine gradient may be rationalized in terms of the possible reasons based on characteristic binding energies of functional groups given in Table 2. First, the cross-linking structure was formed by the condensation of Si–OH between that on the surface of $SiO_2$ particles and from hydrolysis of MAPTIPS. Second, the hydrogen bond was existed between surface Si–OH and –OH of the functional monomer HEMA. The non-linear scaling behavior will have a great negative impact on the ability of the flouroalkyl polymer chains to diffuse to the air/polymer interface [5], leading to the gradient of fluorine only to take effect on the shallow surface layer because of the faster velocity of cross-linking than that of fluorine enriching.

**Table 5**
Various roughness parameters for samples of Fig. 4.

| Factors | Film of recipe 4 | Film of recipe 6 | Film of recipe 7 | Film of recipe 8 |
|---|---|---|---|---|
| $S_q$ (nm) | 4.0 | 35.6 | 20.2 | 15.3 |
| $R_a$ (nm) | 4.9 | 27.9 | 15.8 | 11.9 |
| $S_z$ (nm) | 30 | 198 | 167 | 116 |
| $R$ | 1.02 | 1.83 | 1.32 | 1.28 |

The contact angle on film surface was determined by two important factors which are chemical compositions and surface structure. In an effort to gain information of the surface in the process of film formation, AFM was employed to observe the surface morphologies of different fluoropolymer films. The parameters of root-mean-square ($S_q$), roughness average ($R_a$), 10 point height ($S_z$) and roughness factor ($R = 1 + S_{dr}$) [17] were obtained from AFM software analyses as shown in Table 5.

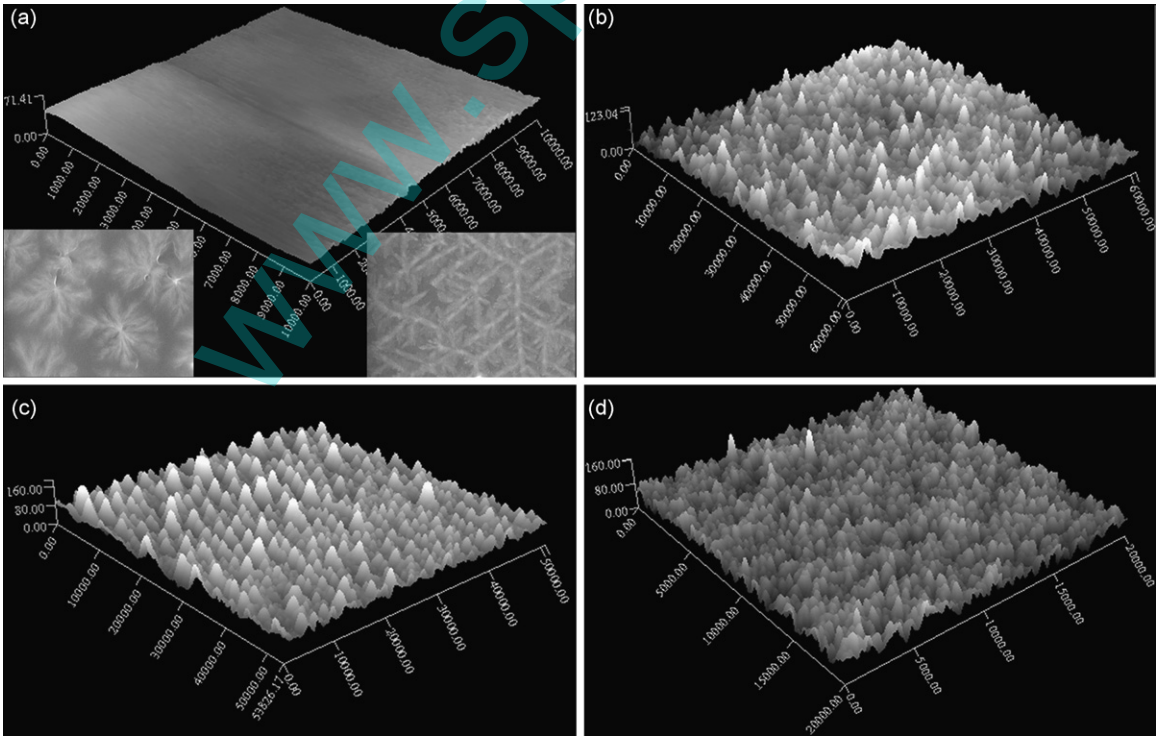


**Fig. 4.** AFM images of different fluorinated emulsion films (a, DFMA–MAPTIPS–acrylates; b, containing modified $SiO_2$ and MAPTIPS; c, containing raw $SiO_2$ and MAPTIPS; d, containing raw $SiO_2$ without MAPTIPS, all samples have same fluorine content).

The smooth surface morphology of film containing DFMA and MAPTIPS but without $SiO_2$ was shown in Fig. 4a, exhibiting low roughness as summarized in Table 5. The dandelion-shaped particles crossing into branches-network can be seen clearly on the surface by SEM in Fig. 4a, indicating phase separation between fluorinated and hydrocarbon components occurred even though the repulsion between them is weak. On the surface of the film (recipe 8) containing MAPTIPS and modified $SiO_2$, there was a quantity of summits (Fig. 4b) and the values of roughness factors increased though the modified $SiO_2$ particles have good compatibility with organic polymers due to good encapsulation. The summits on the surface of sample 7, however, seem to be higher (Fig. 4c) than that on the surface of sample 8, and the value of roughness factors increased slightly too. It can be elucidated that more fluorine-containing groups and silica enriched on the surface contacting the air even though the phase separation between organic and inorganic phases is not very strong because of the improvement of compatibility for the presence of MAPTIPS. As a result of the condensation between the silanol functional groups on $SiO_2$ surface and that from hydrolysis of MAPTIPS, it facilitated the enrichment of $SiO_2$ particles on the surface of film when silicon orientating on the surface. However, most silica aggregates are covered by a layer of the fluorinated polymer, leading to the increase of fluorine.

Comparing the difference of surface morphology between samples 6 and 7, the summits on the surface and the magnitude of roughness parameters of the film containing raw $SiO_2$ in the lack of MAPTIPS increased apparently (Fig. 4d). It can be inferred that during the casting process, silica particles moved to the surface and prevented the coalescence of polymer latex, which increased the micro-roughness and pits on the surface. This also confirmed that the phase separation between inorganic and organic is crucial to promote $SiO_2$ to congregate on the surface when the raw $SiO_2$ particles were not encapsulated and the fluorine content on the surface was confined. The results of AFM characterization were in good agreement with that of XPS.

## 4. Conclusion

Inorganic–organic hybrid latex containing fluorinated copolymer has been prepared using multistage emulsion polymerization techniques. The particle morphologies of a variety of latexes were examined by transmission electron microscopy, and it was found that the fluoroacrylates may encapsulate on the core by controlling appropriate conditions. Results of XPS showed that the content of fluorine in the outmost surface is higher than the calculated value and the fluorinated side chains enrich and orient toward the surface. Although the contact angle for water on the fluorinated film with HFBA is much low, the XPS data is still consistent with the behavior of low surface energy materials orienting at the polymer–air interface. This effect may be enhanced by MAPTIPS, irrespective of the presence of $SiO_2$, because it has a similar property of propensity on the surface with fluoroacrylates. The analysis of XPS and AFM has shown that the gradient distribution of fluorine concentration from depth profile in the film increased when the silica particles were present together with MAPTIPS because of aggregation on the surface of silica particles covered by fluoropolymer. But when raw $SiO_2$ particles were added solely, phase separation between organic and inorganic plays an important role because of failed encapsulation so that the orientation on the surface of fluorine was restrained. The surface topography is the result of the joint effect of fluorine-containing chains and silica particles in the very surface. Moreover, the results of contact angle measurement support the conclusion from surface morphology analysis. No matter what kind of $SiO_2$ particles is used, the gradient of fluorine has a sharp transformation in a small depth from surface because of increased cross-linking density. These results are benefit for preparing hydrophobic film while keeping good adhesion, hardness and mechanical strength.

## References


[1] J.D. Jeyaprakash, S. Samuel, J. Rühe, A facile photochemical surface modification technique for the generation of microstructured fluorinated surfaces, Langmuir 20 (2004) 10080.
[2] I.J. Park, S.B. Lee, C.K. Choi, Surface properties of the fluorine-containing graft copolymer of poly((perfluoroalkyl)ethyl methacrylate)-*g*-poly(methyl methacrylate), Macromolecules 31 (1998) 7555.
[3] J. Genzer, K. Efimenko, Creating long-lived super hydrophobic polymer surfaces through mechanically assembled monolayers, Science 290 (2000) 2130.
[4] F. Bauer, H.J. Gläsel, U. Decker, H. Ernst, A. Freyer, E. Hartmann, V. Sauerland, R. Mehnert, Trialkoxysilane grafting onto nanoparticles for the preparation of clear coat polyacrylate systems with excellent scratch performance, Progress in Organic Coatings 47 (2003) 147.
[5] R.R. Thomas, D.R. Anton, W.F. Graham, M.J. Darmon, B.B. Sauer, K.M. Stika, D.G. Swartzfager, Preparation and surface properties of acrylic polymers containing fluorinated monomers, Macromolecules 30 (1997) 2883.
[6] M. Hikita, K. Tanaka, T. Nakamura, T. Kajiyama, A. Takahara, Super-liquid-repellent surfaces prepared by colloidal silica nanoparticles covered with fluoroalkyl groups, Langmuir 21 (2005) 7299.
[7] ZhG. Yu, ZhB. Zhang, Q.L. Yuan, ShK. Ying, Surface analysis of coating based on novel water-diluted fluorinated polymer/silica hybrids, Advances in Polymer Technology 21 (2002) 268.
[8] W. Stöber, A. Fink, E. Bohn, Journal of Colloid Interface and Science 26 (1968) 62.
[9] S.L. Westcott, S.J. Oldenburg, Lee T. Randall, N.J. Halas, Formation and adsorption of clusters of gold nanoparticles onto functionalized silica nanoparticle surfaces, Langmuir 14 (1998) 5396.
[10] Ph. Espiard, A. Guyot, Poly(ethyl acrylate) latexes encapsulating nanoparticles of silica 2: grafting process onto silica, Polymer 36 (1995) 4391.
[11] A.L. Qu, X.F. Wen, P.H. Pi, J. Cheng, Z.R. Yang, Synthesis of composite particles through emulsion polymerization based on silica/fluoroacrylate-siloxane using anionic reactive and nonionic surfactants, Journal of Colloid Interface and Science 317 (2008) 62.
[12] S.L. Huang, W.K. Chin, W.P. Yang, Structural characteristics and properties of silica/poly(2-hydroxyethyl methacrylate) (PHEMA) nanocomposites prepared by mixing colloidal silica or tetraethyloxysilane (TEOS) with PHEMA, Polymer 46 (2005) 1865.
[13] J. Tsibouklis, P. Graham, P.J. Eaton, J.R. Smith, T.G. Nevell, J.D. Smart, R.J. Ewen, Poly(perfluoroalkyl methacrylate) film structures: surface organization phenomena, surface energy determinations, and force of adhesion measurements, Macromolecules 33 (2000) 8460.
[14] C.M. Kassis, J.K. Steehler, D.E. Betts, Z. Guan, T.J. Romack, J.M. DeSimone, R.W. Linton, XPS studies of fluorinated acrylate polymers and block copolymers with polystyrene, Macromolecules 29 (1996) 3247.
[15] R.R. Thomas, K.G. Lloyd, K.M. Stika, L.E. Stephans, G.S. Magallanes, V.L. Dimonie, E.D. Sudol, M.S. El-Aasser, Low free energy surfaces using blends of fluorinated acrylic copolymer and hydrocarbon acrylic copolymer latexes, Macromolecules 33 (2000) 8828.
[16] E. Bourgeat-Lami, J. Lang, Encapsulation of inorganic particles by dispersion polymerization in polar media 1. Silica nanoparticles encapsulated by polystyrene, Journal of Colloid Interface and Science 197 (1998) 293.
[17] J. Peltonen, M. Järn, S. Areva, M. Linden, J.B. Rosenholm, Topographical parameters for specifying a three-dimensional surface, Langmuir 20 (2004) 9428.